

CO₂-forced climate thresholds during the Phanerozoic

Dana L. Royer *

Department of Earth and Environmental Sciences, Wesleyan University, Middletown, CT 06459-0139, USA

Received 4 August 2005; accepted in revised form 30 November 2005

Abstract

The correspondence between atmospheric CO₂ concentrations and globally averaged surface temperatures in the recent past suggests that this coupling may be of great antiquity. Here, I compare 490 published proxy records of CO₂ spanning the Ordovician to Neogene with records of global cool events to evaluate the strength of CO₂-temperature coupling over the Phanerozoic (last 542 my). For periods with sufficient CO₂ coverage, all cool events are associated with CO₂ levels below 1000 ppm. A CO₂ threshold of below ~500 ppm is suggested for the initiation of widespread, continental glaciations, although this threshold was likely higher during the Paleozoic due to a lower solar luminosity at that time. Also, based on data from the Jurassic and Cretaceous, a CO₂ threshold of below ~1000 ppm is proposed for the initiation of cool non-glacial conditions. A pervasive, tight correlation between CO₂ and temperature is found both at coarse (10 my timescales) and fine resolutions up to the temporal limits of the data set (million-year timescales), indicating that CO₂, operating in combination with many other factors such as solar luminosity and paleogeography, has imparted strong control over global temperatures for much of the Phanerozoic.

© 2006 Elsevier Inc. All rights reserved.

1. Introduction

Carbon dioxide (CO₂) is an important greenhouse gas, and its role in regulating global surface temperatures has been recognized for over a century (Arrhenius, 1896; Chamberlin, 1899). It is now generally accepted that the 36% rise in atmospheric CO₂ since 1860 (280–380 ppm) is partly responsible for the concomitant rise in global surface temperatures (Tett et al., 1999; Crowley, 2000b; Barnett et al., 2001; Mitchell et al., 2001; Jones et al., 2003; Karl and Trenberth, 2003; Karoly et al., 2003; Miller et al., 2004). Moreover, ice core records indicate a strong coupling between CO₂ and temperature for at least the last 650,000 years (Petit et al., 1999; Siegenthaler et al., 2005). Given this observed, positive relationship between CO₂ and temperature and the physical laws that govern it, an a priori expectation is that the CO₂-temperature link is of great antiquity.

1.1. Temperature records

A significant obstacle to testing the antiquity of the CO₂-temperature link is generating accurate records of CO₂ and temperature for times in Earth's past that are tens to hundreds-of-million years old. The most robust measure of global temperature from before the Pleistocene is the presence vs. absence of large continental icesheets (Hambrey and Harland, 1981; Frakes et al., 1992) because it is difficult to envision large volumes of ice coexisting with globally warm temperatures (e.g., Crowley and North, 1991). Direct indicators of continental glaciation that are commonly preserved in the rock record include abraded rock surfaces, such as polished or striated pavements, chattermarks, and tillites (diamictites [unsorted sediments with a large range in grain size] deposited directly by glaciers) (Hambrey and Harland, 1981; Eyles et al., 1983). Indirect evidence for large continental ice masses include rapid eustasy (>100 m/my) that cannot be accommodated by tectonic motion alone (Rowley and Markwick, 1992), however these higher-order features in sea level records have been called into question (e.g., Eyles, 1993; Markwick and Rowley, 1998). Erratics (outsized clast in a fine-grained

* Fax: +1 860 685 3651.

E-mail address: droyer@wesleyan.edu

matrix; also known as dropstones) are often invoked as indicators of cold climates (Frakes and Francis, 1988; Frakes et al., 1992; Price, 1999) because the most common mode for rafting such clasts out to sea is ice; indeed, these deposits are often called ice-rafted debris (IRD) (e.g., Frakes and Francis, 1988). However, animals, algae, and trees are also capable of rafting decimeter-to-meter sized clasts long distances (>400 km; Markwick and Rowley, 1998); erratics, particularly isolated deposits lacking corroborative evidence, should not be taken as indicators of glaciation or even cold climates.

Despite the power of glacial records as a temperature proxy, they are explicitly qualitative and are less helpful during ice-free periods when global temperatures can range from cool to hot (e.g., Crowley et al., 1986, 1987). For these reasons, quantitative temperature records derived from the $\delta^{18}\text{O}$ of marine carbonates (e.g., Veizer et al., 2000) are attractive. However, a problem with these records is that the secular 8‰ increase across the Phanerozoic has not been adequately explained; this is important because the amplitude of the second-order oscillations, which are often assumed to reflect temperature, is only ~4‰. A second problem is that seawater pH influences the $\delta^{18}\text{O}$ of carbonate (Spero et al., 1997; Zeebe, 2001); this is critical for studies tracking CO_2 and temperature because CO_2 imparts strong control over seawater pH, such that if pH is not taken into account (e.g., Veizer et al., 2000) the CO_2 -temperature link is artificially weakened (Royer et al., 2004). Third, original carbonate is commonly altered diagenetically, leading to falsely cool temperatures (Pearson et al., 2001); however, this issue is less problematic for short-term events (Crowley and Zachos, 2000). Finally, for planktic $\delta^{18}\text{O}$ records it is important to have geographically widespread coverage for a given time slice before making inferences about global surface temperatures (e.g., MacLeod et al., 2005). Nevertheless, despite these drawbacks, benthic paleotemperatures are generally good integrators of globally averaged surface temperatures and rapid changes in $\delta^{18}\text{O}$ typically reflect either temperature or ice volume (e.g., Zachos et al., 2001). Also, in many cases Mg/Ca ratios provide an independent paleothermometer and help to deconvolve the temperature and ice volume signals (e.g., Lear et al., 2000).

A second, more qualitative paleothermometer that has been used to track ancient global climate states is the presence of glendonite carbonate nodules (Frakes et al., 1992; Price, 1999; but see Markwick and Rowley, 1998). Glendonite is considered a pseudomorph of ikaite ($\text{CaCO}_3 \cdot 6\text{H}_2\text{O}$), which is stable only near 0 °C (Sherman and Smith, 1985). The presence of glendonite nodules therefore implies cool conditions (at least regionally), but not necessarily permanent ice.

1.2. CO_2 records

Pre-Pleistocene records of CO_2 are derived from either proxies or geochemical carbon cycle models. The

geochemical models track fluxes of carbon entering and exiting the atmosphere; models that are appropriate for million-year timescales focus on processes that influence atmospheric CO_2 on 10^5 to 10^6 year timescales such as burial of organic carbon, chemical weathering of Ca–Mg silicates, and volcanic outgassing. The best-regarded model of this class that predicts CO_2 for the full Phanerozoic is GEOCARB, which has a time-step of 10 my (Berner and Kothavala, 2001); this means that CO_2 fluctuations operating at timescales shorter than 10 my may not influence GEOCARB. It should be noted that long-term carbon cycle models are not restricted a priori to 10 my time steps, and can be used to explore patterns across brief intervals at higher resolutions (Kump et al., 1999; Berner, 2005), providing the required input data are available at the equivalent resolution.

All CO_2 proxies operate on the same principle: a feature of the Earth system that covaries with CO_2 in the present-day and that can be reliably measured in the rock record is quantified for the present-day and then applied to the past. The following proxies have emerged over the past 15 years as the most robust (see Royer et al., 2001 for more details): the $\delta^{13}\text{C}$ of pedogenic minerals (Cerling, 1991; Yapp and Poths, 1992); the stomatal densities and indices in plants (Van der Burgh et al., 1993; McElwain and Chaloner, 1995); the $\delta^{13}\text{C}$ of long-chained alkenones in haptophytic algae (Pagani et al., 1999); the $\delta^{11}\text{B}$ of marine carbonate (Pearson and Palmer, 1999; but see Pagani et al., 2005); and the $\delta^{13}\text{C}$ of liverworts (Fletcher et al., 2005).

1.3. Phanerozoic CO_2 and temperature: What do the records say?

Studies that track CO_2 and temperature over the Phanerozoic typically find that periods of low CO_2 correlate with long-lived, extensive continental glaciations while periods of high CO_2 do not overlap with these glaciations (Berner, 1991, 1994; Berner and Kothavala, 2001; Crowley and Berner, 2001; Royer et al., 2004). These results contrast with one study that did not find a strong coupling between Phanerozoic CO_2 and temperature (Veizer et al., 2000), but this is because the temperature proxy, the $\delta^{18}\text{O}$ of shallow marine carbonate, was not corrected for seawater pH (Royer et al., 2004); once corrected, the temperature data correlate strongly with both the record of continental glaciation and atmospheric CO_2 (Royer et al., 2004).

These previous studies primarily focused on broad, multi-million-year patterns between CO_2 and temperature. This was a consequence of the coarse time resolution of GEOCARB (10 my), a lack of CO_2 proxy data, and difficulties in placing data in a finely resolved stratigraphic framework, particularly for terrestrial sections. Nevertheless, a positive correlation between CO_2 and temperature at 10-million-year timescales emerged (Crowley and Berner, 2001; Royer et al., 2004). Here, I scrutinize the Phanerozoic records of CO_2 and temperature in finer detail, often approaching million-year timescales. This improved

level of analysis is possible because of a more extensive CO₂ proxy database (490 individual records vs. 372 in Royer et al. (2004), a 32 % increase), new analyses for the timing of the Permo-Carboniferous glaciation (Isbell et al., 2003), improved records of Mesozoic and early Cenozoic climates (e.g., Dromart et al., 2003a; Tripathi et al., 2005), and a new geologic timescale (Gradstein et al., 2004). The primary goal of this study is to assess the strength of CO₂-temperature coupling at million-year timescales. In particular, global climate models (GCMs) calibrated to mid-Cenozoic conditions predict that permanent ice initiates when CO₂ levels drop below 560–1120 ppm (2–4× pre-industrial levels; DeConto and Pollard, 2003; Pollard and DeConto, 2005). Is this prediction borne out in the rock record? And more broadly, are globally cool periods associated with lower CO₂ concentrations than warm periods?

2. Methods

Four hundred and ninety records of Phanerozoic CO₂ were compiled from the literature, spanning the Late Ordovician to early Pleistocene; errors in CO₂ and age were estimated when possible (see [electronic annex](#)). Most individual CO₂ data points are based on replicate samples. CO₂ coverage is good for the late Carboniferous (Pennsylvanian) to Permian, Middle Triassic, and latest Cretaceous (Maastrichtian) to Neogene; coverage is relatively sparse for before the Pennsylvanian, the Permian-Triassic boundary interval, and Late Cretaceous (excluding the Maastrichtian) (Fig. 1A). To provide an independent comparison, the proxy record of CO₂ is compared to the CO₂ output from the most recent GEOCARB geochemical model (GEOCARB III; Berner and Kothavala, 2001).

Records of globally cool climates were placed into one of two categories: (1) periods with direct evidence for geographically widespread continental ice (polished or striated pavements, chattermarks, and tillites); (2) periods with indirect evidence for continental ice (rapid eustasy and rapid changes in marine $\delta^{18}\text{O}$) and/or geographically widespread evidence for cool climates ($\delta^{18}\text{O}$ records,

glendonite nodules, and, when corroborated with supporting evidence, erratics). Periods with direct evidence for continental ice represent the coldest Earth states, while periods

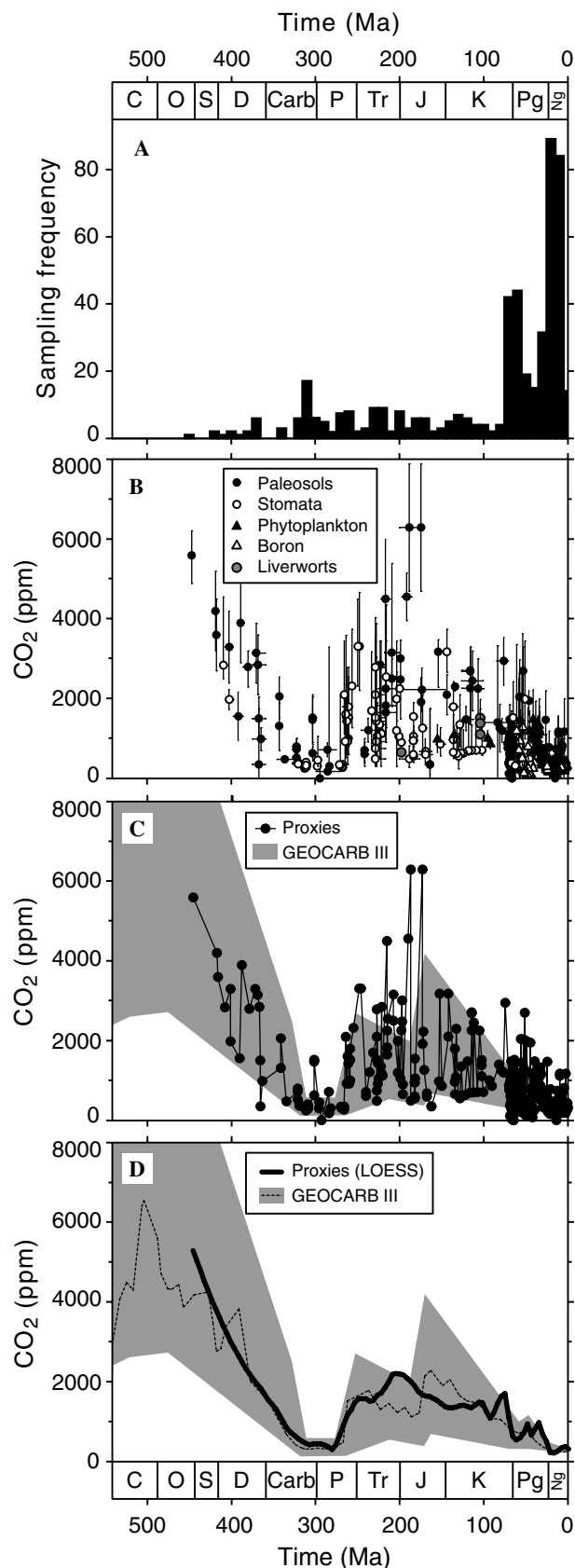


Fig. 1. Atmospheric CO₂ through the Phanerozoic. (A) Temporal distribution of the CO₂ proxy record, expressed in 10 my time blocks. (B) Phanerozoic CO₂ proxy record, categorized by method. Errors in CO₂ estimates and ages are given when available. See [electronic annex](#) for further details. (C) The same CO₂ record as in (B), but expressed as a time series without error bars. Also plotted are the range of reasonable CO₂ predictions from the geochemical model GEOCARB III (Berner and Kothavala, 2001). (D) Comparison of the best-guess predictions of GEOCARB III (dashed line) with a smoothed representation of the proxy record (solid line; locally weighted regression [LOESS]; sampling proportion = 0.1; polynomial degree = 2) that best matches the temporal resolution of GEOCARB (~10 my time-step). This approach differs from Royer et al. (2004), who expressed the proxy record in 10 my time-steps, because here the ages of the GEOCARB output have been calibrated to the timescale of Gradstein et al. (2004) and no longer follow an even 10 my time-step.

with evidence for widespread cooling and/or indirect or equivocal evidence for permanent ice represent cool Earth states. An important distinction between the cool and cold Earth states is that the cool intervals have no unequivocal evidence for permanent ice. Many original literature sources were incorporated in this analysis, but the compilations of Frakes et al. (1992), Eyles (1993), Crowell (1999), Price (1999), and Isbell et al. (2003) proved most valuable. All CO₂ and climate records were calibrated to the timescale of Gradstein et al. (2004); chronostratigraphic nomenclature also follows Gradstein et al. (2004). Formal statistical analyses are not presented here: a comparison between CO₂ from proxies and geochemical models was presented by Royer et al. (2004) but cannot be updated here owing to the uneven time-steps of the revised data (see Fig. 1 caption). Statistical comparisons between CO₂ and temperature are also not possible because the temperature data presented here are largely derived from regional studies, and so cannot be directly equated to global mean temperatures.

3. Results and discussion

3.1. Fidelity of Phanerozoic CO₂ record

All 490 CO₂ proxy records and their attendant errors are plotted in Fig. 1B, sorted by method; Fig. 1C plots the data as a time series without error bars. When viewed at the scale of the Phanerozoic (Fig. 1B and C), the overarching pattern is of high CO₂ (4000+ ppm) during the early Paleozoic, a decline to present-day levels by the Pennsylvanian (~320 Ma), a rise to high values (1000–3000 ppm) during the Mesozoic, then a decline to the present-day. These broad patterns are discernible even when the errors of individual data points (Fig. 1B) are taken into account.

When the CO₂ proxy record is compared to the range of reasonable CO₂ predictions from the GEOCARB III model (gray shaded region in Fig. 1C), it is clear that the vast majority of proxy data fall within this uncertainty envelope. This provides support for the fidelity of the proxy record. To explore this comparison further, Fig. 1D plots the ‘best-guess’ predictions of GEOCARB III against a locally weighted regression (LOESS) of the proxy data, where the LOESS is fitted to match the time-step of GEOCARB III. Again, a positive correlation is evident between these two independent records, and is consistent with previous analyses (Crowley and Berner, 2001; Royer et al., 2004). We can say with growing confidence that the broad, multi-million-year patterns of CO₂ during much of the Phanerozoic are known.

If the GEOCARB and proxy CO₂ records are used to calculate radiative forcing (see Fig. 2 caption for details), the same general patterns remain: radiative forcing is the same or weaker than pre-industrial conditions only during the two intervals of widespread, long-lived glaciation, the Permo-carboniferous and late Cenozoic (Fig. 2). The main difference between the radiative forcing (Fig. 2) and CO₂

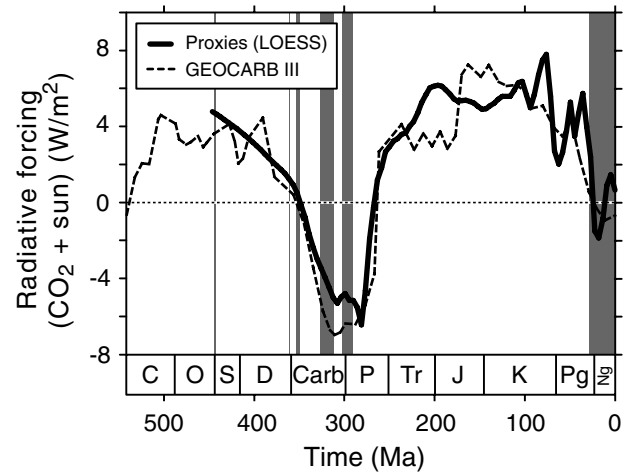


Fig. 2. Radiative forcing through the Phanerozoic. Radiative forcing is derived following the protocol of Crowley (2000a) and the radiative transform expression for CO₂ of Myhre et al. (1998). For the calculation, the CO₂ records from Fig. 1D are used and solar luminosity is assumed to linearly increase starting at 94.5% present-day values. Values are expressed relative to pre-industrial conditions (CO₂ = 280 ppm; solar luminosity = 342 W/m²); a reference line of zero is given for clarity. The dark shaded bands correspond to periods with strong evidence for geographically widespread ice (see Section 2 for details).

(Fig. 1D) records is that radiative forcing is comparatively low during the early Paleozoic owing to a weaker solar constant at that time.

3.2. Correlating CO₂ to temperature: Late Ordovician glaciation (Hirnantian; 445.6–443.7 Ma)

There is unequivocal evidence for a widespread but brief Gondwanan glaciation during the end-Ordovician (Hirnantian Stage; 445.6–443.7 Ma). Several reports argue for a longer interval of ice centered on the Ordovician–Silurian boundary (e.g., 58 my in Frakes et al., 1992), and alpine glaciers may have indeed persisted in Brazil and Bolivia into the early Silurian (Crowell, 1999), but most recent studies demonstrate that the dominant glacial phase was restricted to the Hirnantian (Brenchley et al., 1994, 2003; Paris et al., 1995; Crowell, 1999; Sutcliffe et al., 2000).

There is one CO₂ data point available that is close in age to this glaciation, and it suggests very high CO₂ levels (5600 ppm; see Fig. 3A; Yapp and Poets, 1992, 1996); moreover, GEOCARB III predicts high CO₂ levels at this time (~4200 ppm; see Fig. 1D). Apparently, this event presents a critical test for the CO₂-temperature paradigm (e.g., Van Houten, 1985; Crowley and Baum, 1991). However, it is unclear what CO₂ levels were during this event. The single proxy record is Ashgillian in age, which spans the Hirnantian but also most of the preceding Stage (450–443.7 Ma); if the CO₂ data point dates to the pre-Hirnantian Ashgillian, then this is consistent with a well-described mid-Ashgillian global warm event (Boucot et al., 2003; Fortey and Cocks, 2005). As for the insensitivity of GEOCARB III to the glaciation, this is unsurprising given the brief duration of the event. Kump et al. (1999)

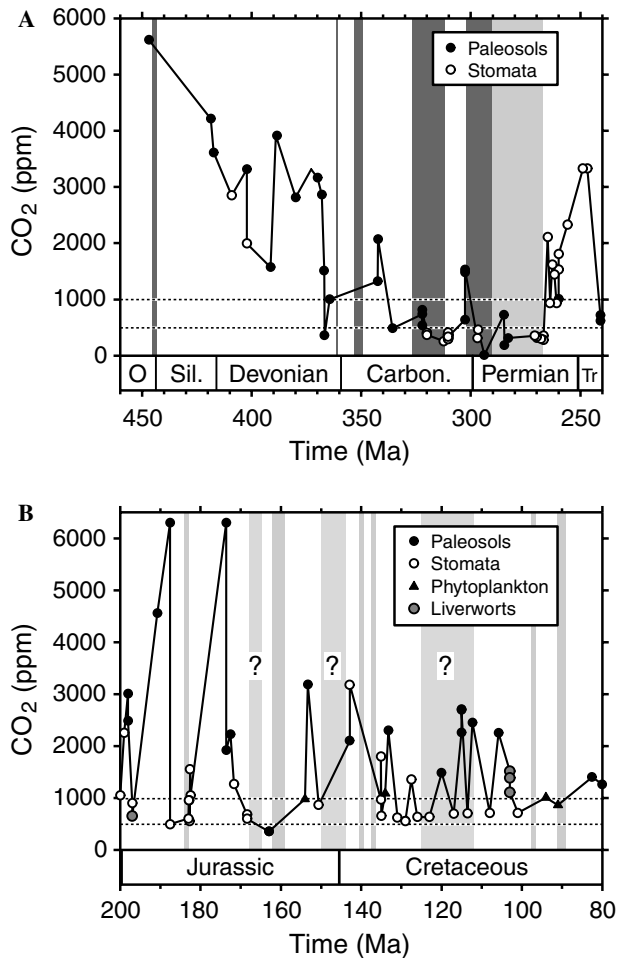


Fig. 3. CO₂ and temperature records for the (A) Late Ordovician to early Triassic (460–240 Ma) and (B) Jurassic to late Cretaceous (200–80 Ma). The CO₂ record is derived from Fig. 1B. Cold periods with strong evidence for geographically widespread ice are marked with dark shaded bands. Cool-to-cold periods with indirect or equivocal evidence for ice (see Section 2 for details) are marked with light shaded bands. The horizontal dashed lines at 1000 and 500 ppm CO₂ represent the proposed CO₂ thresholds for, respectively, the initiation of globally cool events and full glacials. Note that the scaling of the time axis differs between the two panels.

addressed this shortcoming by applying a high-resolution carbon cycle model across the Hirnantian; their model predicts that CO₂ levels declined from ~5000 to 3000 ppm.

Although the strength of CO₂-temperature coupling cannot be presently tested for this event, it is worthwhile to examine what the CO₂ threshold for initiating a glaciation at this time may be. Global climate models calibrated to mid-Cenozoic conditions suggest a threshold of 560–1120 ppm (DeConto and Pollard, 2003; Pollard and DeConto, 2005), however during the Late Ordovician surface conditions were different, most notably in having an ~4% lower solar constant. A consequence of this decreased luminosity is that if all other thermal forcings were held constant, the CO₂ threshold for initiating a glaciation would be higher. A simple analysis of radiative forcing (see Fig. 2) suggests that if the CO₂-ice threshold for the

present-day Earth is 500 ppm, the equivalent threshold during the Late Ordovician would be 3000 ppm. Importantly, global climate models and energy balance models calibrated to Late Ordovician conditions also predict a CO₂-ice threshold of between 2240 and 3920 ppm (Crowley and Baum, 1991, 1995; Gibbs et al., 1997, 2000; Kump et al., 1999; Poussart et al., 1999; Herrmann et al., 2003, 2004). This prediction awaits confirmation from the proxy record.

3.3. Correlating CO₂ to temperature: Late Devonian and early Carboniferous glaciations (361–349 Ma)

There is evidence for two widespread but brief continental glaciations during the Late Devonian and early Carboniferous (Crowell, 1999). Similar to the Permo-Carboniferous glaciation (section 3.4), these are principally Gondwanan events, occurring when eastern South America and central Africa crossed the South Pole (Powell and Li, 1994). The Late Devonian glaciation is restricted to the middle *Siphonodella praesulcata* conodont zone of the Famennian (361.4–360.6 Ma) and may consist of two distinct pulses (Crowell, 1999); rock evidence for this event comes from Bolivia and Brazil (Crowell, 1999; Isbell et al., 2003). The early Carboniferous glaciation appears to span the mid- to late Tournaisian (353–349 Ma; Crowell, 1999) based on sediments from Bolivia, Brazil, and north Africa; however, some authors consider this evidence equivocal (Isbell et al., 2003).

Unfortunately, no CO₂ records are currently available for either of these events. Moderately high levels of CO₂ are found 3 my before the Late Devonian glaciation (1000 ppm) and 7 my after the early Carboniferous glaciation (1300 ppm; see Fig. 3A). If the late Cenozoic and Permo-Carboniferous glaciations are considered analogues, and if changes in solar luminosity are taken into account (see Section 3.2; Fig. 2), then CO₂ levels probably needed to drop below 2000 ppm to initiate the formation of permanent ice; however, at present this hypothesis cannot be tested. Curiously, there is some evidence for ice near the Frasnian–Famennian boundary (374.5 Ma; Crowell, 1999; Isbell et al., 2003), a time of rapidly declining CO₂ levels (3300–350 ppm; see Fig. 3A).

3.4. Correlating CO₂ to temperature: Permo-Carboniferous glaciation (326–267 Ma)

The longest and most extensive Phanerozoic glaciation occurred during the Carboniferous and Permian, during which time Antarctica and Australia drifted across the South Pole (Frakes et al., 1992; Eyles, 1993; Crowell, 1999). Traditionally, this glaciation is considered to have lasted from the base of the Namurian to the top of the Kazanian (326–267 Ma; e.g., Frakes et al., 1992), some 60 my in length. Broadly speaking, this cold interval corresponds with low levels of atmospheric CO₂ (Fig. 1C and D; see also Crowley and Berner, 2001; Royer et al., 2004).

However, there is a distinct period of elevated CO₂ (1500 ppm) centered at 300 Ma (Fig. 3A); based on the traditional age placement of the Permo-Carboniferous glaciation, this period of high CO₂ weakens claims for CO₂-temperature coupling across the event.

A recent reassessment of the timing and duration of this glaciation (Isbell et al., 2003) largely rectifies this CO₂-temperature disparity. Instead of a continuous, 60 my long record of ice, Isbell et al. (2003) argue for two shorter but discrete phases. The older phase begins at the base of the Namurian and ends in the early Westphalian (326.4–311.7 Ma); direct, unequivocal evidence for ice at this time comes from western South America and eastern Australia. The second cold phase commences during the early Stephanian and terminates during the mid-Sakmarian (302–290 Ma; see also Wopfner, 1999); evidence for ice during this interval is geographically more extensive, coming from South America, Africa, Antarctica, Australia, and India. According to Isbell et al. (2003), there is no convincing evidence for ice between these two phases (311.7–302 Ma). Post-dating the second icy phase, there is sparse and sporadic evidence for ice (direct evidence: diamictites with striated clasts; indirect evidence: erratics) until the Kazanian (290–267 Ma; Isbell et al., 2003). This final phase is therefore not considered a full glacial; global temperatures were likely warmer relative to the two full glacial phases.

The strength of CO₂-temperature coupling during the Permo-Carboniferous glaciation can now be reevaluated in light of this new temporal framework. CO₂ is consistently low during the first glacial phase (326.4–311.7 Ma), with most data <500 ppm (Fig. 3A). Interestingly, CO₂ may have been <500 ppm for 10–15 my preceding the onset of permanent ice (Fig. 3A). Between the two glacial phases, CO₂ coverage is sparse, but a period of high CO₂ (1500 ppm) falls at the end of this interglacial phase. Concomitant with the initiation of the second glacial phase, CO₂ quickly drops to below 500 ppm and remains at these levels for the duration of the cold phase. After the termination of the second icy phase (290 Ma), the Earth shifted to a cool state until 267 Ma. During this cool phase, CO₂ remained below 500 ppm except for at least one excursion to levels between 500 and 1000 ppm. Directly after the termination of this cool phase, CO₂ increased to 1000+ ppm and remained high until the early Triassic (Fig. 3A).

These patterns are largely consistent with a strong coupling between CO₂ and temperature: CO₂ levels were high before and after the Permo-Carboniferous glaciation, and generally low during the event. An investigation into some of the finer-scale patterns of CO₂ and temperature provide a compelling case for positive CO₂-temperature coupling during most or all of this event.

3.5. Correlating CO₂ to temperature: Early Jurassic to Cretaceous cool pulses (184–66.5 Ma)

There is no direct evidence for permanent ice during the Mesozoic and early Cenozoic (Frakes et al., 1992; Eyles,

1993; Markwick and Rowley, 1998; Price, 1999). Indeed, for large spans of this interval the Earth was warmer than the present-day (e.g., Vakhrameev, 1991; Norris and Wilson, 1998; Wilson and Norris, 2001; Zachos et al., 2001; Huber et al., 2002; Norris et al., 2002; Wilson et al., 2002; Schouten et al., 2003). This general paradigm of a global ‘hothouse’ is consistent with the CO₂ record, which broadly shows moderately high to high values (1000+ ppm) during the Mesozoic and early Cenozoic (Fig. 1C and D; see also Crowley and Berner, 2001; Royer et al., 2004) and high radiative forcings (Fig. 2).

However, superimposed on this record of warmth is mounting evidence for cooler climates. For example, Frakes et al. (1992) consider the middle Jurassic to early Cretaceous (Bajocian to mid-Albian; 171.6–106 Ma) a time of cool non-glacial conditions with high-latitude seasonal ice. As I outline below, further scrutiny of the paleotemperature record reveals that there were multiple discrete cool events from at least the early Jurassic to late Cretaceous (Pliensbachian to Maastrichtian; 184–66.5 Ma), each only lasting <3 my in length. Thus, the most plausible climate history for the Jurassic and Cretaceous is one dominated by warm climates but punctuated by brief (<3 my; typically <1 my) cool pulses.

3.5.1. Late Pliensbachian (184–183 Ma)

There is moderately strong evidence for globally cool temperatures during the Late Pliensbachian (184–183 Ma). Eyles (1993) and Price (1999) argue for an increase in the frequency of glendonite nodules and erratics as well as a drop in sea level, while Rosales et al. (2004) present δ¹⁸O and Mg/Ca records from belemnites that indicate a short-term cooling in the Tethys sea. CO₂ coverage across this event is comparatively good (see Fig. 3B): 4 my before the event, CO₂ levels plummeted from very high (6300 ppm) to low (500 ppm) values. During the final phases of the cool event (183 Ma), CO₂ concentrations were still low (500–600 ppm), but rose to higher values (1500 ppm) shortly thereafter. CO₂ appears to have modulated this cool event.

3.5.2. Bathonian (167.7–164.7 Ma) and late Callovian to middle Oxfordian (162–159 Ma)

A strong case exists for globally cool temperatures during the Late Callovian to Middle Oxfordian (162–159 Ma) based on an extensive survey of marine temperatures (Dromart et al., 2003a,b; Lécuyer et al., 2003), a putative drop in sea level (Dromart et al., 2003a,b; but see Hallam, 2001), and the distribution of reefs (Cecca et al., 2005). An increase in the burial rate of organic matter at this time suggests that this cool event was forced by declining CO₂ concentrations (Dromart et al., 2003a,b). CO₂ proxies validate this prediction: CO₂ levels exceeded 1000 ppm before and after the event, but were very low (350 ppm) at its onset (Fig. 3B). Furthermore, there is some evidence for cool climates during the Bathonian (167.7–164.7 Ma; Price, 1999), which also occurs within this interval of low CO₂ (Fig. 3B).

3.5.3. Valanginian (140.5–139.5 Ma, 137.5–136.5 Ma)

Stoll and Schrag (1996) provide marine strontium data that are consistent with two large, rapid drops in sea level reported by Haq et al. (1987) during the Valanginian (140.5–139.5 and 137.5–136.5 Ma). Corroborating evidence for cool climates at this time comes from marine $\delta^{18}\text{O}$ data (Stoll and Schrag, 1996; Erba et al., 2004) and the increased frequency of erratics, diamictites, and glendonites (Frakes et al., 1992; Price, 1999). There are currently no CO₂ data spanning these events, but high CO₂ levels (2000+ ppm) were present both before and after the events (Fig. 3B). Moreover, CO₂ was moderately low (650 ppm) shortly after the termination of the second cool event (135 Ma). Although more CO₂ data are needed, the current patterns are suggestive of CO₂-temperature coupling.

3.5.4. Tithonian to early Berriasian (150–144 Ma) and Aptian (125.0–112.0 Ma)

Price (1999) provides some evidence for cool climates (erratics, diamictites, and glendonites) during the Tithonian to early Berriasian (“Volgian”; 150–144 Ma) and Aptian (125–112 Ma). These putative cool events are longer than the other Jurassic and Cretaceous cool pulses, but they have most likely been artificially smeared by poor dating control (Price, 1999). Nonetheless, the CO₂ record indicates a drop in CO₂ during the Tithonian–Berriasian event (Fig. 3B). CO₂ is more variable during the Aptian; if CO₂ and temperature were coupled, then the Aptian must not have been uniformly cool, instead punctuated by several brief cool periods that correspond with the documented low CO₂ periods (<1000 ppm; see Fig. 3B). For example, the marine paleotemperature record of Steuber et al. (2005) is consistent with a cool interval during the early Aptian.

3.5.5. mid-Cenomanian (97.5–96.5 Ma) and mid-Turonian (91–89 Ma)

Miller et al. (2003, 2004) present evidence for glacio-eustatic control of sea level during the mid-Cenomanian (top of CC9 nannofossil zone; 97.5–96.5 Ma) and mid-Turonian (top of CC12 nannofossil zone; 91–89 Ma) that is consistent with the Haq et al. (1987) sea level curve. Support for two brief cool pulses comes from marine $\delta^{18}\text{O}$ records (Frakes, 1999; Stoll and Schrag, 2000; Miller et al., 2003, 2004). The marine paleotemperature estimates of Wilson et al. (2002) and Steuber et al. (2005) are also consistent with a mid-Turonian cooling. CO₂ data are sparse through this interval, but in general CO₂ appears to have been moderately low (<1000 ppm; Fig. 3B); in particular, moderately low CO₂ conditions (860 ppm) were present at the onset of the mid-Turonian event.

3.5.6. Maastrichtian (71.6–69.6 Ma; 67.5–66.5 Ma; 65.6–65.5 Ma)

Multiple lines of evidence point towards brief global cooling events near the Campanian–Maastrichtian boundary (71.6–69.6 Ma), mid-Maastrichtian (67.5–66.5 Ma),

and end-Maastrichtian (65.6–65.5 Ma). The first event is supported by rapid shifts in both sea level (Haq et al., 1987; Miller et al., 1999, 2003, 2004) and the $\delta^{18}\text{O}$ of marine carbonate (Pirrie and Marshall, 1990; Barrera and Savin, 1999; Frakes, 1999; Miller et al., 2004), as well as terrestrial temperature reconstructions (Parrish and Spicer, 1988). Rapid shifts in sea level (Haq et al., 1987; Miller et al., 2003, 2004) and marine $\delta^{18}\text{O}$ records (MacLeod and Huber, 1996; Barrera and Savin, 1999; Huber et al., 2002; Miller et al., 2004) support the mid-Maastrichtian event, while geographically widespread marine (Wilf et al., 2003) and terrestrial (Nordt et al., 2003; Wilf et al., 2003) temperature reconstructions support the very brief (~0.1 my) end-Maastrichtian event.

The CO₂ record for the Maastrichtian is data-rich, spanning from below 500 to ~1500 ppm; CO₂ before the first cool event in the late Campanian was apparently very high (3000 ppm; Fig. 3B). A closer look at the Maastrichtian CO₂ and temperature records show a fine-scale structure that is consistent with strong CO₂-temperature coupling: CO₂ during the three cool events remained below 1000 ppm, while outside of these events CO₂ often exceeded 1000 ppm (Fig. 3B).

3.5.7. Jurassic and Cretaceous summary

Although there is no definitive evidence for permanent ice during the Jurassic and Cretaceous, a wide variety of alternative temperature proxies provide a compelling case for CO₂-temperature coupling at million-year timescales. These brief periods of globally cool climates and low CO₂ do not conflict with GEOCARB III (which predicts a steady decline in CO₂ from ~2200 to 800 ppm across this interval; see Fig. 1D) owing to the model’s coarse 10 my temporal resolution.

3.6. Correlating CO₂ to temperature: Late Cenozoic glaciation (34 Ma–present)

The best-documented period of continental glaciation is the most recent glaciation that began in the late Eocene and continues to the present day (e.g., Crowley and North, 1991; Frakes et al., 1992; Eyles, 1993; Ruddiman, 2000). Broadly speaking, global surface temperatures cooled with the onset of glaciation (Zachos et al., 1992, 2001; Lear et al., 2000). A rich CO₂ record derived from four independent methods spans this glaciation (Fig. 3). These data provide a highly consistent signal of low CO₂ concentrations (<500 ppm; see also Fig. 1C for Phanerozoic context of data). One exception may be the late Oligocene (~25 Ma), a known time of global warming (Zachos et al., 2001), where several CO₂ data points cluster above 500 ppm (Fig. 4). CO₂ levels today are probably higher than they have been for the last 25 my; the few data that exceed 500 ppm during this interval are derived from the paleosol method and have associated errors of at least ± 500 ppm (Ekart et al., 1999; Royer et al., 2001), and so are statistically indistinguishable from the low CO₂

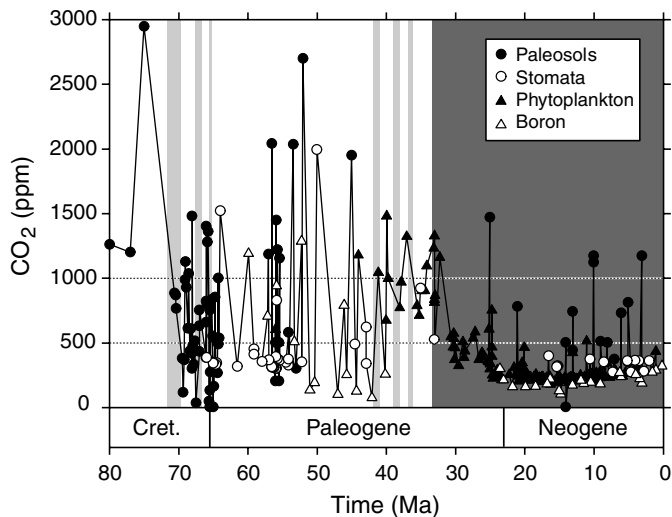


Fig. 4. CO₂ and temperature records for the late Cretaceous to present day (80–0 Ma). The CO₂ record is derived from Fig. 1B. Cold periods with strong evidence for geographically widespread ice are marked with dark shaded bands. Cool-to-cold periods with indirect or equivocal evidence for ice (see Section 2 for details) are marked with light shaded bands; such periods supported by only weak evidence are annotated with a question mark. The horizontal dashed lines at 1000 and 500 ppm CO₂ represent the proposed CO₂ thresholds for, respectively, the initiation of globally cool events and full glacials.

records. The late Eocene to present-day is the clearest example in the Phanerozoic of a long-term positive coupling between CO₂ and temperature (see also Crowley and Berner, 2001; Royer et al., 2004).

Most sea level reconstructions imply that transient ice-sheets developed multiple times before switching to a permanent glacial state near the Eocene-Oligocene boundary (Haq et al., 1987; Browning et al., 1996). Tripathi et al. (2005) provide a strong, albeit indirect, case for three short-lived glaciations at 42–41 Ma, 39–38 Ma, and 36.5–36 Ma based on independent reconstructions of sea level, temperature, and calcite compensation depth. The CO₂ record indicates moderately high CO₂ levels (1200 ppm) at 44 Ma, dropping to low levels (<500 ppm) just before the onset of the first cool event at 42 Ma (Fig. 4). This pattern of CO₂ (<1000 ppm during cool events and >1000 ppm elsewhere) generally persists across the remaining two events (Fig. 4).

3.7. Future work

The science of reconstructing pre-Pleistocene CO₂ concentrations has rapidly developed in recent years: 88% of the CO₂ records presented here were published after 1998. This rich record has allowed for statistically meaningful comparisons between CO₂ and temperature at multi-million-year timescales (Royer et al., 2004) and, as presented here, investigations at finer resolutions. Nevertheless, there are still gaps in both the CO₂ and temperature records. For example, the three short-lived Paleozoic glaciations (Late Ordovician, Late Devonian, and early

Carboniferous) presently do not have CO₂ coverage (Fig. 3A). Also, coverage during the Permo-Carboniferous glaciation is good, but any given period within this event is covered by only one proxy method (paleosol or stomatal method); given that all of the stomatal-based reconstructions are low during this period, it would be worthwhile to cross-check them with the paleosol method.

The Triassic is the only Phanerozoic Period with no evidence (direct or indirect) for ice (e.g., Frakes et al., 1992); correspondingly, CO₂ levels are typically high, with the smoothed CO₂ record reaching a peak near the Triassic–Jurassic boundary before steadily declining to the present-day (Fig. 1D). However, when viewed in finer detail, the CO₂ record reveals two brief periods of low CO₂ (<800 ppm) during the first half of the Triassic (~241 and 228 Ma; see Figs. 1C and 3A). The first low CO₂ event is consistent with a high-resolution isotope mass balance model (1 my time-step) that predicts a short-lived increase in the burial rate of organic matter at this time (Berner, 2005); the output of this model ends at 240 Ma and does not overlap with the younger 228 Ma event. If the rest of the Phanerozoic is taken as an analogue, an expectation would be for both low periods of CO₂ to correspond with cool climates; this expectation awaits testing. Similarly, low CO₂ conditions (<1000 ppm) were present during the earliest Jurassic (Hettangian; 199.6–196.5 Ma) and during brief periods of the mid-Cretaceous (Barremian, Aptian, and Albian; 130.0–99.6 Ma). An increase in the frequency of erratics and diamictites is reported for the Hettangian (Price, 1999), and some evidence exists for cool mid-Cretaceous climates (Frakes et al., 1992; Sellwood et al., 1994; Pirrie et al., 1995; Price, 1999; see also Section 3.5.4), but further work is warranted.

Finally, despite having a rich CO₂ and temperature record, the Paleocene to early Eocene is a climate enigma: globally averaged surface temperatures were significantly warmer than the present day (Zachos et al., 2001) and there is no convincing evidence for ice (Frakes et al., 1992), but CO₂ estimates range from <300 to >2000 ppm (Fig. 1C). It is doubtful that the excursions to low CO₂ correspond to cool pulses in a manner similar to the rest of the Phanerozoic. Instead, it is possible that the boundary conditions of the Earth system were sufficiently different at this time, for example with respect to paleogeography, latent heat transport (cf. Ufnar et al., 2004 for Cretaceous example), or increased residence time of atmospheric methane (cf. Valdes et al., 2005 for Pleistocene example).

4. Conclusion

Atmospheric CO₂ is positively correlated with globally averaged surface temperatures for most of the Phanerozoic. This pattern has been previously shown at coarse 10-million-year timescales and is demonstrated here at finer resolutions (one million to five million-year timescales). The two longest-lived Phanerozoic glaciations during the Permo-Carboniferous and late Cenozoic are the only

Phanerozoic intervals associated with consistently low levels of CO₂ (<500 ppm). This pattern supports predictions from global climate models for a CO₂-ice threshold of 560–1120 ppm (DeConto and Pollard, 2003; Pollard and DeConto, 2005).

A growing number of cool, putatively non-glacial periods have been identified in the Phanerozoic. A pervasive pattern with these events is their brevity, typically <3 my and often <1 my. These cool periods are marked by either low-to-moderate levels of CO₂ (<1000 ppm) or no CO₂ coverage. Crucially, none of the cool periods are associated with CO₂ levels exceeding 1000 ppm.

Many factors are important in controlling the average surface temperature of the Earth, including solar luminosity, albedo, distribution of continents and vegetation, orbital parameters, and other greenhouse gases. The message of this study is not that atmospheric CO₂ is always the dominant forcing (see Section 3.7 for an early Paleogene example). Instead, given the variety of factors that can influence global temperatures, it is striking that such a consistent pattern between CO₂ and temperature emerges for many intervals of the Phanerozoic. This correspondence suggests that CO₂ can explain in part the patterns of globally averaged temperatures during the Phanerozoic.

Acknowledgments

I dedicate this contribution to Bob Berner, whose creative outlook and attention to detail have provided me with a lifetime of inspiration. I thank D. Beerling, B. Fletcher, M. Haworth, and M. Pagani for access to their CO₂ data and D. Beerling, T. Crowley, L. Kump, I. Montañez, and S. O'Connell for helpful comments on the manuscript.

Associate editor: Lee Kump

Appendix A. Supplementary data

Supplementary data associated with this article can be found, in the online version, at doi:10.1016/j.gca.2005.11.031.

References

- Arrhenius, S., 1896. On the influence of carbonic acid in the air upon the temperature on the ground. *Philos. Mag. J. Sci.* **41**, 237–275.
- Barnett, T.P., Pierce, D.W., Schnur, R., 2001. Detection of anthropogenic climate change in the world's oceans. *Science* **292**, 270–274.
- Barrera, E., Savin, S.M., 1999. Evolution of late Campanian–Maastrichtian marine climates and oceans. In: Barrera, E., Johnson, C.C. (Eds.), *Evolution of the Cretaceous Ocean–Climate System Geological Society of America Special Paper 332*, Boulder. pp. 245–282.
- Berner, R.A., 1991. A model for atmospheric CO₂ over Phanerozoic time. *Am. J. Sci.* **291**, 339–376.
- Berner, R.A., 1994. GEOCARB II: a revised model of atmospheric CO₂ over Phanerozoic time. *Am. J. Sci.* **294**, 56–91.
- Berner, R.A., 2005. The carbon and sulfur cycles and atmospheric oxygen from middle Permian to middle Triassic. *Geochim. Cosmochim. Acta* **69**, 3211–3217.
- Berner, R.A., Kothavala, Z., 2001. GEOCARB III: A revised model of atmospheric CO₂ over Phanerozoic time. *Am. J. Sci.* **301**, 182–204.
- Boucot, A.J., Jia-yu, R., Xu, C., Scotese, C.R., 2003. Pre-Hirnantian Ashgill climatically warm event in the Mediterranean region. *Lethaia* **36**, 119–132.
- Brenchley, P.J., Carden, G.A., Hints, L., Kaljo, D., Marshall, J.D., Martma, T., Meidla, T., Nölvak, J., 2003. High-resolution stable isotope stratigraphy of Upper Ordovician sequences: constraints on the timing of bioevents and environmental changes associated with mass extinction and glaciation. *Geol. Soc. Am. Bull.* **115**, 89–104.
- Brenchley, P.J., Marshall, J.D., Carden, G.A.F., Robertson, D.B.R., Long, D.G.F., Meidla, T., Hints, L., Anderson, T.F., 1994. Bathymetric and isotopic evidence for a short-lived Late Ordovician glaciation in a greenhouse period. *Geology* **22**, 295–298.
- Browning, J.V., Miller, K.G., Pak, D.K., 1996. Global implications of lower to middle Eocene sequence boundaries on the New Jersey coastal plain: the icehouse cometh. *Geology* **24**, 639–642.
- Cecca, F., MartinGarin, B., Marchand, D., Lathuiliere, B., Bartolini, A., 2005. Paleoclimatic control of biogeographic and sedimentary events in Tethyan and peri-Tethyan areas during the Oxfordian (Late Jurassic). *Palaeogeogr. Palaeoclimatol. Palaeoecol.* **222**, 10–32.
- Cerling, T.E., 1991. Carbon dioxide in the atmosphere: evidence from Cenozoic and Mesozoic paleosols. *Am. J. Sci.* **291**, 377–400.
- Chamberlin, T.C., 1899. An attempt to frame a working hypothesis of the cause of glacial periods on an atmospheric basis. *J. Geol.* **7**, 545–584.
- Crowell, J.C., 1999. *Pre-Mesozoic ice ages: their bearing on understanding the climate system*. Geological Society of America Memoir 192, Boulder.
- Crowley, T.J., 2000a. Carbon dioxide and Phanerozoic climate. In: Huber, B.T., MacLeod, K.G., Wing, S.L. (Eds.), *Warm Climates in Earth History*. Cambridge University Press, Cambridge, pp. 425–444.
- Crowley, T.J., 2000b. Causes of climate change over the past 1000 years. *Science* **289**, 270–277.
- Crowley, T.J., Baum, S.K., 1991. Toward reconciliation of Late Ordovician (~440 Ma) glaciation with very high CO₂ levels. *J. Geophys. Res.* **96**, 22597–22610.
- Crowley, T.J., Baum, S.K., 1995. Reconciling Late Ordovician (440 Ma) glaciation with very high (14×) CO₂ levels. *J. Geophys. Res.* **100**, 1093–1101.
- Crowley, T.J., Berner, R.A., 2001. CO₂ and climate change. *Science* **292**, 870–872.
- Crowley, T.J., North, G.R., 1991. *Paleoclimatology*. Oxford University Press, New York.
- Crowley, T.J., Zachos, J.C., 2000. Comparison of zonal temperature profiles for past warm time periods. In: Huber, B.T., MacLeod, K.G., Wing, S.L. (Eds.), *Warm Climates in Earth History*. Cambridge University Press, Cambridge, pp. 50–76.
- Crowley, T.J., Short, D.A., Mengel, J.G., North, G.R., 1986. Role of seasonality in the evolution of climate during the last 100 million years. *Science* **231**, 579–584.
- Crowley, T.J., Mengel, J.G., Short, D.A., 1987. Gondwanaland's seasonal cycle. *Nature* **329**, 803–807.
- DeConto, R.M., Pollard, D., 2003. Rapid Cenozoic glaciation of Antarctica induced by declining atmospheric CO₂. *Nature* **421**, 245–249.
- Dromart, G., Garcia, J.P., Gaumet, F., Picard, S., Rousseau, M., Atrops, F., Lécuyer, C., Sheppard, S.M.F., 2003a. Perturbations of the carbon cycle at the Middle/Late Jurassic transition: geological and geochemical evidence. *Am. J. Sci.* **303**, 667–707.
- Dromart, G., Garcia, J.-P., Picard, S., Atrops, F., Lécuyer, C., Sheppard, S.M.F., 2003b. Ice age at the Middle-Late Jurassic transition? *Earth Planet. Sci. Lett.* **213**, 205–220.
- Ekart, D.D., Cerling, T.E., Montañez, I.P., Tabor, N.J., 1999. A 400 million year carbon isotope record of pedogenic carbonate: implications for paleoatmospheric carbon dioxide. *Am. J. Sci.* **299**, 805–827.
- Erba, E., Bartolini, A., Larson, R.L., 2004. Valanginian Weissert oceanic anoxic event. *Geology* **32**, 149–152.

- Eyles, N., 1993. Earth's glacial record and its tectonic setting. *Earth-Sci. Rev.* **35**, 1–248.
- Eyles, N., Eyles, C.H., Miall, A.D., 1983. Lithofacies types and vertical profile modes; an alternative approach to the description and environmental interpretation of glacial diamict sequences. *Sedimentology* **30**, 393–410.
- Fletcher, B.J., Beerling, D.J., Royer, D.L., Brentnall, S.J., 2005. Fossil bryophytes as recorders of ancient CO₂ levels: Experimental evidence and a Cretaceous case study. *Glob. Biogeochem. Cyc.* **19**, GB3012. doi:10.1029/2005GB002495.
- Fortey, R.A., Cocks, L.R.M., 2005. Late Ordovician global warming—the Boda event. *Geology* **33**, 405–408.
- Frakes, L.A., 1999. Estimating the global thermal state from Cretaceous sea surface and continental temperature data. In: Barrera, E., Johnson, C.C. (eds.) *Evolution of the Cretaceous Ocean-Climate System*. Geological Society of America Special Paper 332, Boulder, pp. 49–57.
- Frakes, L.A., Francis, J.E., 1988. A guide to Phanerozoic cold polar climates from high-latitude ice-rafting in the Cretaceous. *Nature* **333**, 547–549.
- Frakes, L.A., Francis, J.E., Syktus, J.I., 1992. *Climate Modes of the Phanerozoic*. Cambridge University Press, Cambridge.
- Gibbs, M.T., Barron, E.J., Kump, L.R., 1997. An atmospheric pCO₂ threshold for glaciation in the Late Ordovician. *Geology* **25**, 447–450.
- Gibbs, M.T., Bice, K.L., Barron, E.J., Kump, L.R., 2000. Glaciation in the early Paleozoic 'greenhouse': the roles of paleogeography and atmospheric CO₂. In: Huber, B.T., MacLeod, K.G., Wing, S.L. (Eds.), *Warm Climates in Earth History*. Cambridge University Press, Cambridge, pp. 386–422.
- Gradstein, F.M., Ogg, J.G., Smith, A.G., 2004. *A Geologic Timescale 2004*. Cambridge University Press, Cambridge.
- Hallam, A., 2001. A review of the broad pattern of Jurassic sea level changes and their possible causes in the light of current knowledge. *Palaeogeogr. Palaeoclimatol. Palaeoecol.* **167**, 23–37.
- Hambrey, M.J., Harland, W.B., 1981. *Earth's Pre-Pleistocene Glacial Record*. Cambridge University Press, Cambridge.
- Haq, B.U., Hardenbol, J., Vail, P.R., 1987. Chronology of fluctuating sea levels since the Triassic (250 million years ago to present). *Science* **235**, 1156–1167.
- Herrmann, A.D., Patzkowsky, M.E., Pollard, D., 2003. Obliquity forcing with 8–12 times preindustrial levels of atmospheric pCO₂ during the Late Ordovician glaciation. *Geology* **31**, 485–488.
- Herrmann, A.D., Patzkowsky, M.E., Pollard, D., 2004. The impact of paleogeography, pCO₂, poleward ocean heat transport and sea level change on global cooling during the Late Ordovician. *Palaeogeogr. Palaeoclimatol. Palaeoecol.* **206**, 59–74.
- Huber, B.T., Norris, R.D., MacLeod, K.G., 2002. Deep-sea paleotemperature record of extreme warmth during the Cretaceous. *Geology* **30**, 123–126.
- Isbell, J.L., Miller, M.F., Wolfe, K.L., Lenaker, P.A., 2003. Timing of late Paleozoic glaciation in Gondwana: Was glaciation responsible for the development of northern hemisphere cyclothem? In: Chan, M.A., Archer, A.W. (eds.) *Extreme Depositional Environments: Mega end Members in Geologic Time*. Geological Society of America Special Paper 340, Boulder, pp. 5–24.
- Jones, G.S., Tett, S.F.B., Stott, P.A., 2003. Causes of atmospheric temperature change 1960–2000: a combined attribution analysis. *Geophys. Res. Lett.* **3** (5), 1128. doi:10.1029/2002GL016377.
- Karl, T.R., Trenberth, K.E., 2003. Modern global climate change. *Science* **302**, 1719–1723.
- Karoly, D.J., Braganza, K., Stott, P.A., Arblaster, J.M., Meehl, G.A., Broccoli, A.J., Dixon, K.W., 2003. Detection of a human influence on North American Climate. *Science* **302**, 1200–1203.
- Kump, L.R., Arthur, M.A., Patzkowsky, M.E., Gibbs, M.T., Pinkus, D.S., Sheenan, P.M., 1999. A weathering hypothesis for glaciation at high atmospheric pCO₂ during the Late Ordovician. *Palaeogeogr. Palaeoclimatol. Palaeoecol.* **152**, 173–187.
- Lear, C.H., Elderfield, H., Wilson, P.A., 2000. Cenozoic deep-sea temperatures and global ice volumes from Mg/Ca in benthic foraminiferal calcite. *Science* **287**, 269–272.
- Lécuyer, C., Picard, S., Garcia, J.-P., Sheppard, S.M.F., Grandjean, P., Dromart, G., 2003. Thermal evolution of Tethyan surface waters during the Middle-Late Jurassic: evidence from δ¹⁸O values of marine fish teeth. *Paleoceanography* **1** (3), 1076. doi:10.1029/2002PA000863.
- MacLeod, K.G., Huber, B.T., 1996. Reorganization of deep ocean circulation accompanying a Late Cretaceous extinction event. *Nature* **380**, 422–425.
- MacLeod, K.G., Huber, B.T., Isaza-Londoño, C., 2005. North Atlantic warming during global cooling at the end of the Cretaceous. *Geology* **33**, 437–440.
- Markwick, P.J., Rowley, D.B., 1998. The geological evidence for Triassic to Pleistocene glaciations: implications for eustasy. In: Pindell, J.L., Drake, C.L. (eds.), *Paleogeographic Evolution and Non-Glacial Eustasy, Northern South America*. Society for Sedimentary Geology (SEPM) Special Publication No. 58, Tulsa, pp. 17–43.
- McElwain, J.C., Chaloner, W.G., 1995. Stomatal density and index of fossil plants track atmospheric carbon dioxide in the Palaeozoic. *Ann. Bot.* **76**, 389–395.
- Miller, K.G., Barrera, E., Olsson, R.K., Sugarman, P.J., Savin, S.M., 1999. Does ice drive early Maastrichtian eustasy? *Geology* **27**, 783–786.
- Miller, K.G., Sugarman, P.J., Browning, J.V., Kominz, M.A., Hernández, J.C., Olsson, R.K., Wright, J.D., Feigenson, M.D., Van Sickle, W., 2003. Late Cretaceous chronology of large, rapid sea level changes: Glacioeustasy during the greenhouse world. *Geology* **31**, 585–588.
- Miller, K.G., Sugarman, P.J., Browning, J.V., Kominz, M.A., Olsson, R.K., Feigenson, M.D., Hernández, J.C., 2004. Upper Cretaceous sequences and sea level history, New Jersey Coastal Plain. *Geol. Soc. Am. Bull.* **116**, 368–393.
- Mitchell, J.F.B., Karoly, D.J., Hegerl, G.C., Zwiers, F.W., Allen, M.R., Marengo, J., 2001. Detection of climate change and attribution of causes. In: Houghton, J.T. et al. (Eds.), *Climate Change 2001: The Scientific Basis. Contribution of Working Group I to the Third Assessment Report of the Intergovernmental Panel on Climate Change*. Cambridge University Press, New York, pp. 695–738.
- Myhre, G., Highwood, E.J., Shine, K.P., Stordal, F., 1998. New estimates of radiative forcing due to well mixed greenhouse gases. *Geophys. Res. Lett.* **25**, 2715–2718.
- Nordt, L., Atchley, S., Dworkin, S., 2003. Terrestrial evidence for two greenhouse events in the latest Cretaceous. *GSA Today* **13** (12), 4–9.
- Norris, R.D., Wilson, P.A., 1998. Low-latitude sea-surface temperatures for the mid-Cretaceous and the evolution of planktic foraminifera. *Geology* **26**, 823–826.
- Norris, R.D., Bice, K.L., Magno, E.A., Wilson, P.A., 2002. Jiggling the tropical thermostat in the Cretaceous hothouse. *Geology* **30**, 299–302.
- Pagani, M., Freeman, K.H., Arthur, M.A., 1999. Late Miocene atmospheric CO₂ concentrations and the expansion of C₄ grasses. *Science* **285**, 876–879.
- Pagani, M., Lemarchand, D., Spivack, A., Gaillardet, J., 2005. A critical evaluation of the boron isotope-pH proxy: the accuracy of ancient ocean pH estimates. *Geochim. Cosmochim. Acta* **69**, 953–961.
- Paris, F., Elaouad-Debbaj, Z., Jaglin, J.C., Massa, D., Oulebsir, L., 1995. Chitinozoans and Late Ordovician glacial events on Gondwana. In: Cooper, J.D., Droser, M.L., Finney, S.C. (eds.) *Ordovician Odyssey: Short Papers for the Seventh International Symposium on the Ordovician System*. The Pacific Section Society for Sedimentary Geology (SEPM), Fullerton, pp. 171–176.
- Parrish, J.T., Spicer, R.A., 1988. Late Cretaceous terrestrial vegetation: a near-polar temperature curve. *Geology* **16**, 22–25.
- Pearson, P.N., Palmer, M.R., 1999. Middle Eocene seawater pH and atmospheric carbon dioxide concentrations. *Science* **284**, 1824–1826.
- Pearson, P.N., Ditchfield, P.W., Singano, J., Harcourt-Brown, K.G., Nicholas, C.J., Olsson, R.K., Shackleton, N.J., Hall, M.A., 2001. Warm tropical sea surface temperatures in the Late Cretaceous and Eocene epochs. *Nature* **413**, 481–487.
- Petit, J.R., Jouzel, J., Raynaud, D., Barkov, N.I., Barnola, J.-M., Basile, I., Bender, M., Chappellaz, J., Davis, M., Delaygue, G., Delmotte, M., Kotlyakov, V.M., Legrand, M., Lipenkov, V.Y., Lorius, C., Pépin, L., Ritz, C., Saltzman, E., Stievenard, M., 1999. Climate and atmospheric

- history of the past 420,000 years from the Vostok ice core, Antarctica. *Nature* **399**, 429–436.
- Pirrie, D., Marshall, J.D., 1990. High-paleolatitude Late Cretaceous paleotemperatures: New data from James Ross Island, Antarctica. *Geology* **18**, 31–34.
- Pirrie, D., Doyle, P., Marshall, J.D., Ellis, G., 1995. Cool Cretaceous climates: new data from the Albian of Western Australia. *J. Geol. Soc. Lond.* **152**, 739–742.
- Pollard, D., DeConto, R.M., 2005. Hysteresis in Cenozoic Antarctic ice-sheet variations. *Glob. Planet. Change* **45**, 9–21.
- Poussart, P.F., Weaver, A.J., Barnes, C.R., 1999. Late Ordovician glaciation under high atmospheric CO₂: a coupled model analysis. *Paleoceanography* **14**, 542–558.
- Powell, C.M., Li, Z.X., 1994. Reconstruction of the Panthalassan margin of Gondwanaland. In: Veevers, J.J., Powell, C.M. (eds.). *Permian-Triassic Pangean basins and foldbelts along the Panthalassan Margin of Gondwanaland*. Geological Society of America Memoir 184, Boulder. pp. 5–9.
- Price, G.D., 1999. The evidence and implications of polar ice during the Mesozoic. *Earth Sci. Rev.* **48**, 183–210.
- Rosales, I., Quesada, S., Robles, S., 2004. Paleotemperature variations of Early Jurassic seawater recorded in geochemical trends of belemnites from the Basque-Cantabrian basin, northern Spain. *Palaeogeogr. Palaeoclimatol. Palaeoecol.* **203**, 253–275.
- Rowley, D.B., Markwick, P.J., 1992. Haq et al. eustatic sea level curve: implications for sequestered water volumes. *J. Geol.* **100**, 703–715.
- Royer, D.L., Berner, R.A., Beerling, D.J., 2001. Phanerozoic CO₂ change: evaluating geochemical and paleobiological approaches. *Earth Sci. Rev.* **54**, 349–392.
- Royer, D.L., Berner, R.A., Montañez, I.P., Tabor, N.J., Beerling, D.J., 2004. CO₂ as a primary driver of Phanerozoic climate. *GSA Today* **14** (3), 4–10.
- Ruddiman, W.F., 2000. *Earth's Climate: Past and Future*. W.H. Freeman, New York.
- Schouten, S., Hopmans, E.C., Forster, A., van Breugel, Y., Kuypers, M.M.M., Sinninghe Damsté, J.S., 2003. Extremely high sea-surface temperatures at low latitudes during the middle Cretaceous as revealed by archaeal membrane lipids. *Geology* **31**, 1069–1072.
- Sellwood, B.W., Price, G.D., Valdes, P.J., 1994. Cooler estimates of Cretaceous temperatures. *Nature* **370**, 453–455.
- Sherman, D.J., Smith, A.J., 1985. Ikaite, the parent mineral of jarrowite-type pseudomorphs. *Proc. Geol. Ass.* **96**, 305–314.
- Siegenthaler, U., Stocker, T.F., Monnin, E., Lüthi, D., Schwander, J., Stauffer, B., Raynaud, D., Barnola, J.-M., Fischer, H., Masson-Delmotte, V., Jouzel, J., 2005. Stable carbon cycle-climate relationship during the late Pleistocene. *Science* **310**, 1313–1317.
- Spero, H.J., Bijma, J., Lea, D.W., Bemis, B.E., 1997. Effect of seawater carbonate concentration on foraminiferal carbon and oxygen isotopes. *Nature* **390**, 400–497.
- Steuber, T., Rauch, M., Masse, J.-P., Graaf, J., Malkoč, M., 2005. Low-latitude seasonality of Cretaceous temperatures in warm and cold episodes. *Nature* **437**, 1341–1344.
- Stoll, H.M., Schrag, D.P., 1996. Evidence for glacial control of rapid sea level changes in the Early Cretaceous. *Science* **272**, 1771–1774.
- Stoll, H.M., Schrag, D.P., 2000. High-resolution stable isotope records from the Upper Cretaceous rocks of Italy and Spain: Glacial episodes in a greenhouse planet? *Geol. Soc. Am. Bull.* **112**, 308–319.
- Sutcliffe, O.E., Dowdeswell, J.A., Whittington, R.J., Theron, J.N., Craig, J., 2000. Calibrating the Late Ordovician glaciation and mass extinction by the eccentricity cycles of Earth's orbit. *Geology* **28**, 967–970.
- Tett, S.F.B., Stott, P.A., Allen, M.R., Ingram, W.J., Mitchell, J.F.B., 1999. Causes of twentieth-century temperature change near the Earth's surface. *Nature* **399**, 569–572.
- Tripathi, A., Backman, J., Elderfield, H., Ferretti, P., 2005. Eocene bipolar glaciation associated with global carbon cycle changes. *Nature* **436**, 341–346.
- Ufnar, D.F., González, L.A., Ludvigson, G.A., Brenner, R.L., Witzke, B.J., 2004. Evidence for increased latent heat transport during the Cretaceous (Albian) greenhouse warming. *Geology* **32**, 1049–1052.
- Vakhrameev, V.A., 1991. *Jurassic and Cretaceous Floras and Climates of the Earth*. Cambridge University Press, Cambridge.
- Valdes, P.J., Beerling, D.J., Johnson, C.E., 2005. The ice age methane budget. *Geophys. Res. Lett.* **32**, L02704. doi:10.1029/2004GL021004.
- Van der Burgh, J., Visscher, H., Dilcher, D.L., Kürschner, W.M., 1993. Paleatmospheric signatures in Neogene fossil leaves. *Science* **260**, 1788–1790.
- Van Houten, F.B., 1985. Oolitic ironstones and contrasting Ordovician and Jurassic paleogeography. *Geology* **13**, 722–724.
- Veizer, J., Godderis, Y., François, L.M., 2000. Evidence for decoupling of atmospheric CO₂ and global climate during the Phanerozoic eon. *Nature* **408**, 698–701.
- Wilf, P., Johnson, K.R., Huber, B.T., 2003. Correlated terrestrial and marine evidence for global climate changes before mass extinction at the Cretaceous–Paleogene boundary. *Proc. Natl Acad. Sci. USA* **100**, 599–604.
- Wilson, P.A., Norris, R.D., 2001. Warm tropical ocean surface and global anoxia during the mid-Cretaceous period. *Nature* **412**, 425–429.
- Wilson, P.A., Norris, R.D., Cooper, M.J., 2002. Testing the Cretaceous greenhouse hypothesis using glassy foraminiferal calcite from the core of the Turonian tropics on Demerara Rise. *Geology* **30**, 607–610.
- Wopfner, H., 1999. The early Permian deglaciation event between East Africa and northwestern Australia. *J. Afr. Earth Sci.* **29**, 77–90.
- Yapp, C.J., Poths, H., 1992. Ancient atmospheric CO₂ pressures inferred from natural goethites. *Nature* **355**, 342–344.
- Yapp, C.J., Poths, H., 1996. Carbon isotopes in continental weathering environments and variations in ancient atmospheric CO₂ pressure. *Earth Planet. Sci. Lett.* **137**, 71–82.
- Zachos, J.C., Breza, J.R., Wise, S.W., 1992. Early Oligocene ice-sheet expansion on Antarctica—stable isotope and sedimentological evidence from Kerguelen Plateau, Southern Indian Ocean. *Geology* **20**, 569–573.
- Zachos, J., Pagani, M., Sloan, L., Thomas, E., Billups, K., 2001. Trends, rhythms, and aberrations in global climate 65 Ma to present. *Science* **292**, 686–693.
- Zeebe, R.E., 2001. Seawater pH and isotopic paleotemperatures of Cretaceous oceans. *Palaeogeogr. Palaeoclimatol. Palaeoecol.* **170**, 49–57.